

Breaking of the tetra-maximal neutrino mixing pattern

Newton Nath^{1,*}

¹*Instituto de Física, Universidad Nacional Autónoma de México, A.P. 20-364, Ciudad de México 01000, México.*

We make an attempt to study the present status of the tetra-maximal neutrino mixing (TMM) pattern. It predicts all the three leptonic mixing angles $\theta_{13} \approx 8.4^\circ$, $\theta_{12} \approx 30.4^\circ$, and $\theta_{23} = 45^\circ$ together with the three CP-violating phases $-\delta = \rho = \sigma = 90^\circ$. However, the latest global analysis of neutrino oscillation data prefer relatively higher best-fit value of θ_{12} as well as non-maximal values of both θ_{23}, δ . In order to explain the realistic data, we study the breaking of TMM pattern. We first examine the breaking of TMM due to renormalization group (RG) running effects and then study the impact of explicit breaking terms. We also examine the effect of RG-induced symmetry breaking on the effective Majorana neutrino mass in neutrinoless double beta decay experiments.

I. INTRODUCTION

The discovery of neutrino oscillations [1] have been confirmed by various phenomenal experiments— such as solar, reactor, and, most recently, long baseline experiments. The explanation of neutrino oscillations implies the need for non-zero neutrino masses and the flavor mixing pattern of leptons. In the Standard Model (SM) of particle physics neutrinos are supposed to be massless, the observation of neutrino oscillations thus hint physics beyond the SM. The leptonic flavor mixing pattern is described by 3×3 unitary mixing matrix V (or Pontecorvo-Maki-Nakagawa-Sakata (PMNS) matrix). In the standard PDG parametrization [1], the PMNS matrix V can be decomposed as

$$V = \begin{pmatrix} c_{12}c_{13} & s_{12}c_{13} & s_{13}e^{-i\delta} \\ -s_{12}c_{23} - c_{12}s_{23}s_{13}e^{i\delta} & c_{12}c_{23} - s_{12}s_{23}s_{13}e^{i\delta} & s_{23}c_{13} \\ s_{12}s_{23} - c_{12}c_{23}s_{13}e^{i\delta} & -c_{12}s_{23} - s_{12}c_{23}s_{13}e^{i\delta} & c_{23}c_{13} \end{pmatrix} \begin{pmatrix} e^{i\rho} & 0 & 0 \\ 0 & e^{i\sigma} & 0 \\ 0 & 0 & 1 \end{pmatrix}, \quad (1)$$

where $s_{ij}(c_{ij}) \equiv \sin \theta_{ij}(\cos \theta_{ij})$ for $i < j = 1, 2, 3$, δ denotes the Dirac type CP-violating phase and ρ, σ are the Majorana phases. According to the latest neutrino oscillation results [2], the best-fit values of neutrino oscillations parameters are $\Delta m_{21}^2 = 7.39 \times 10^{-5} \text{eV}^2$, $\Delta m_{31}^2 = 2.525 \times 10^{-3} \text{eV}^2$, $\theta_{12} = 33.82^\circ$, $\theta_{13} = 8.61^\circ$, $\theta_{23} = 48.3^\circ$, and $\delta = 222^\circ$.

Understanding of leptonic flavor mixing pattern is still a mystifying issue in neutrino physics. Flavor symmetry has been very successful in predicting the structure of the leptonic mixing matrix as discussed in [3–7]. Among number of such symmetry bases studies, the lepton mixing matrix which is approximately equal to the tribimaximal (TBM) mixing proposed in [8] turns out to be favored one. Considering the latest neutrino oscillation data [2, 9, 10], the $\mu - \tau$ reflection symmetry, which was originally proposed in Ref. [11] (see Ref. [12] for a latest review and the references therein) leads to $|V_{\mu i}| = |V_{\tau i}|$, (for $i = 1, 2, 3$) as given by Eq. 1 has received a great deal of attention in recent times¹. An immediate consequence of such symmetry is that it predicts the maximal values of the atmospheric mixing angle $\theta_{23} = 45^\circ$ and the Dirac type CP-phase $\delta = \pm 90^\circ$. It also predicts the trivial Majorana CP-phases $\rho, \sigma = 0^\circ, 90^\circ$. However, the mixing angles θ_{13}, θ_{12} are free within this symmetry.

Here we focus on the tetra-maximal leptonic mixing pattern, which was originally proposed by Xing in Ref. [14], in presence of latest oscillation data [2, 9, 10]². The breaking effect of such symmetry has been examined in [15]. The tetra-maximal mixing matrix can be decomposed into four maximal rotations

$$V_0 = P_l \otimes O_{23}(\pi/4, \pi/2) \otimes O_{13}(\pi/4, 0) \otimes O_{12}(\pi/4, 0) \otimes O_{13}(\pi/4, \pi), \quad (2)$$

where $P_l = \text{diag}\{1, 1, i\}$, and $O_{ij}(\theta_{ij}, \delta_{ij})$ is a rotation with the angle θ_{ij} and the phase δ_{ij} in the complex i - j plane for $ij = 12, 23, 13$. The name ‘tetra-maximal mixing’ arises because the mixing matrix V_0 , as given by Eq. 2, can be expressed as a product of four rotation matrices, where all the mixing angles are maximal. Expanded form of V_0 can be written as

* newton@fisica.unam.mx

¹ The importance of such symmetry for upcoming long baseline experiment DUNE has been studied in [13]

² The original idea was to construct neutrino mixing pattern with only two small integers 1 and 2 together with their square roots and the imaginary number i .

$$V_0 = \frac{1}{2} \begin{pmatrix} 1 + \frac{1}{\sqrt{2}} & 1 & 1 - \frac{1}{\sqrt{2}} \\ -\frac{1}{\sqrt{2}} \left[1 + i(1 - \frac{1}{\sqrt{2}}) \right] & 1 + i\frac{1}{\sqrt{2}} & \frac{1}{\sqrt{2}} \left[1 - i(1 + \frac{1}{\sqrt{2}}) \right] \\ -\frac{1}{\sqrt{2}} \left[1 - i(1 - \frac{1}{\sqrt{2}}) \right] & 1 - i\frac{1}{\sqrt{2}} & \frac{1}{\sqrt{2}} \left[1 + i(1 + \frac{1}{\sqrt{2}}) \right] \end{pmatrix}. \quad (3)$$

One can extract three mixing angles as

$$\tan \theta_{12} = 2 - \sqrt{2}, \quad \tan \theta_{23} = 1, \quad \sin \theta_{13} = \frac{1}{4}(2 - \sqrt{2}), \quad (4)$$

where $\theta_{12} \approx 30.4^\circ$, $\theta_{13} \approx 8.4^\circ$, $\theta_{23} = 45^\circ$ and $\delta = -90^\circ$. It also predicts Majorana CP-phases $\rho, \sigma = 90^\circ$. We notice that the predicted θ_{13}, θ_{23} and δ are in excellent agreement with the latest oscillation results [2, 9, 10]. However, mixing angle θ_{12} lies outside the current 3σ range and the predicted value is much smaller than the latest best-fit value. Although the latest T2K [16] results are in good agreement with the symmetry, the current NO ν A [17] results seem to favor non-maximal θ_{23}, δ . Moreover, the latest best-fit values of the global analysis of neutrino oscillations data also favors the same [2, 9, 10].

In this work, we study possible deviations from the tetra-maximal mixing pattern. We aim to explain realistic value of the solar mixing angle θ_{12} together with non-maximal values of the atmospheric mixing angle θ_{23} and the Dirac type CP violating phase δ . In what follows we first study the breaking of tetra-maximal mixing pattern due to the renormalization group equations (RGE). As the flavor symmetries are generally imposed at a superhigh energy scale to address neutrino masses and their flavor mixing at low energies, RGE-running effect may lead to possible corrections and naturally break the exact symmetry. Therefore, we impose the tetra-maximal mixing symmetry at the superhigh energy scale Λ_{TMM} and analyze the deviations due to RGE breaking all the way from Λ_{TMM} down to the electroweak (EW) scale Λ_{EW} . Keeping the current global best-fit results in mind, which prefers θ_{12} considerably large compared to TMM and $\theta_{23} > 45^\circ$ and $\delta < 270^\circ$, we study the correlation among these parameters due to RGE corrections at low energies. Furthermore, whether neutrinos are Majorana or Dirac fermions, is yet unanswered in particle physics³. As the symmetry predicts some trivial values for the Majorana CP-phases, which may also have some significant impact on neutrinoless double beta ($0\nu\beta\beta$) decay experiments. Considering $\rho, \sigma = 90^\circ$ at the energy scale Λ_{TMM} as our initial choice, we study their correlation at low energies due to quantum corrections. We further examine the impact of RGE-induced symmetry breaking on the effective Majorana neutrino mass in $0\nu\beta\beta$ -decay experiments.

Afterwards we perform the breaking of tetra-maximal mixing by introducing explicit breaking term in the leptonic mixing matrix. The explicit breaking parameters have been introduced in such a way that one can explain large solar mixing angle and non-maximal values of atmospheric mixing angle including Dirac type CP violating phase. In next Sec. (II), we examine the impact of RGE-induced symmetry breaking and perform various correlation study to explain the present neutrino oscillation data. Impact of explicit breaking of the tetra-maximal mixing has been addressed in Sec. (III). Finally, we summarize our conclusion in Sec. (IV).

II. SPONTANEOUS BREAKING OF TMM

We have noticed that the mixing angles θ_{13}, θ_{23} predicted by the tetra-maximal mixing pattern are in excellent agreement with the latest neutrino oscillation data, whereas θ_{12} lies outside 3σ [2, 9]. One possible way to explain the most realistic leptonic mixing parameters under the tetra-maximal mixing pattern is to break the symmetry. In general, if one assumes that the concerned mixing pattern is realized under a certain flavor symmetry at superhigh energy scale then the RGE-running will significantly impact the mixing parameters which are measured at low-energies. Thus, the RGE-running effect provides us the possible explanation between the predicted superhigh energy scales mixing parameters to that from the experimentally measured parameters at low energies. In this section, we describe the breaking of tetra-maximal mixing pattern due to RGE-running in context of minimal supersymmetric standard model (MSSM)⁴. Here, we introduce the tetra-maximal mixing pattern at superhigh energy scale Λ_{TMM} ($\equiv 10^{14}$ GeV), much higher compared to electroweak (EW) scale Λ_{EW} ($\sim 10^2$ GeV).

³ E. Majorana first hypothesized that a fermion can be its own antiparticle in 1937 [18].

⁴ Note that the MSSM has been adopted as the theoretical framework at high energies which can serve as a possible ultraviolet extension of the Standard Model.

In Refs. [19], authors have derived the leptonic mixing parameters due to RGE-running within the numerous theoretical frameworks. Considering the leading order approximation, we write down the renormalization group equations for leptonic mixing angles in the MSSM [20] as

$$\begin{aligned}\frac{d\theta_{12}}{dt} &\approx -\frac{y_\tau^2 s_{12}^2 c_{12}^2 s_{23}^2}{8\pi^2 \Delta m_{21}^2} [m_1^2 + m_2^2 + 2m_1 m_2 \cos 2(\rho - \sigma)] , \\ \frac{d\theta_{13}}{dt} &\approx \frac{y_\tau^2 s_{12}^2 c_{12}^2 s_{23}^2 c_{23}^2 m_3}{2\pi^2 \Delta m_{31}^2 (1 + \zeta)} [m_1 \cos(2\rho + \delta) - (1 + \zeta) m_2 \cos(2\sigma + \delta) - \zeta m_3 \cos \delta] , \\ \frac{d\theta_{23}}{dt} &\approx -\frac{y_\tau^2 s_{23}^2 c_{23}^2}{8\pi^2 \Delta m_{31}^2} \left[c_{12}^2 (m_2^2 + m_3^2 + 2m_2 m_3 \cos 2\sigma) + \frac{s_{12}^2 (m_1^2 + m_3^2 + 2m_1 m_3 \cos 2\rho)}{1 + \zeta} \right] ,\end{aligned}\quad (5)$$

with $t = \ln(\mu/\mu_0)$, $\zeta \equiv \Delta m_{21}^2/\Delta m_{31}^2$ and y_τ denotes the Yukawa coupling of the charged-lepton τ .

Similarly, the different CP-violating phases can be given by [20]

$$\begin{aligned}\frac{d\delta}{dt} &= \frac{y_\tau^2 s_{12}^2 c_{12}^2 s_{23}^2 c_{23}^2 m_3 \theta_{13}^{-1}}{2\pi^2 \Delta m_{31}^2 (1 + \zeta)} [(1 + \zeta) m_2 \sin(2\sigma + \delta) - m_1 \sin(2\rho + \delta) + \zeta m_3 \sin \delta] , \\ \frac{d\rho}{dt} &= \frac{y_\tau^2}{8\pi^2} \left\{ m_3 (c_{23}^2 - s_{23}^2) \frac{m_1 s_{12}^2 \sin 2\rho + (1 + \zeta) m_2 c_{12}^2 \sin 2\sigma}{\Delta m_{31}^2 (1 + \zeta)} + \frac{m_1 m_2 c_{12}^2 s_{23}^2 \sin 2(\rho - \sigma)}{\Delta m_{21}^2} \right\} , \\ \frac{d\sigma}{dt} &= \frac{y_\tau^2}{8\pi^2} \left\{ m_3 (c_{23}^2 - s_{23}^2) \frac{m_1 s_{12}^2 \sin 2\rho + (1 + \zeta) m_2 c_{12}^2 \sin 2\sigma}{\Delta m_{31}^2 (1 + \zeta)} + \frac{m_1 m_2 s_{12}^2 s_{23}^2 \sin 2(\rho - \sigma)}{\Delta m_{21}^2} \right\} ,\end{aligned}\quad (6)$$

where both in Eqs. 5, 6 $\mathcal{O}(\theta_{13})$ term have been safely neglected.

In Fig. 1, we show our numerical results due to RGE running for the leptonic mixing parameters. Before moving on to discuss our results, we first illustrate the numerical procedure that has been carried out in this section. In the numerical study, we set the high and low energy boundary scales at $\Lambda_{\text{TMM}} = 10^{14}$ GeV and $\Lambda_{\text{EW}} = 91$ GeV together with $\tan \beta = 30$, respectively. As the tetra-maximal mixing pattern predicts the maximal value of θ_{23} , CP-violating phases ($-\delta = \rho = \sigma = 90^\circ$) along with $\theta_{12} \sim 30.4^\circ$, $\theta_{13} \sim 8.4^\circ$, we fix these values at superhigh energy scale. Furthermore, the mass-squared differences (namely, Δm_{31}^2 and Δm_{21}^2) are scanned over wide ranges with the help of the nested sampling package **MultiNest** program [21] at Λ_{TMM} . We define the Gaussian- χ^2 function in the numerical scan as,

$$\chi^2 = \sum_i \frac{[\xi_i - \bar{\xi}_i]^2}{\sigma_i^2} , \quad (7)$$

where $\xi_i = \{\theta_{12}, \theta_{13}, \theta_{23}, \Delta m_{21}^2, \Delta m_{31}^2\}$ represents the neutrino oscillation parameters at Λ_{EW} . Also, $\bar{\xi}_i$ stands for the best-fit values from the recent global-fit results [2], and σ_i represents the symmetrized 1σ errors.

The best-fit values and the 1σ errors that we have considered in our numerical simulations [2] are $\sin^2 \theta_{12} = 0.310_{-0.012}^{+0.013}$, $\sin^2 \theta_{13} = 0.02241_{-0.00065}^{+0.00065}$, $\sin^2 \theta_{23} = 0.58_{-0.021}^{+0.017}$, $\delta/^\circ = 215_{-29}^{+40}$, $\Delta m_{21}^2 = 7.39_{-0.20}^{+0.21} \times 10^{-5} \text{eV}^2$, $\Delta m_{31}^2 = 2.525_{-0.032}^{+0.033} \times 10^{-3} \text{eV}^2$. Moreover, as the latest neutrino oscillation data favors normal neutrino mass ordering (i.e., $\Delta m_{31}^2 > 0$) with more than 3σ C.L. [2, 9, 10] over inverted neutrino mass ordering (i.e., $\Delta m_{31}^2 < 0$), we concentrate this study considering the former mass ordering and the smallest neutrino mass m_1 is allowed to vary in the range $[0, 0.2]$ eV.

The results describe for mixing parameters in Fig. 1 are in excellent agreement with the analytical expressions as given by Eqs. 5, 6. By inspecting the top row, one can notice that the mixing angle θ_{12} receives the sizable amount of corrections due to RGE induced symmetry breaking than the remaining mixing angles θ_{13} and θ_{23} . This is because of the presence of $\zeta \approx 30$ terms in the expression of θ_{13} and θ_{23} (see Eq. 5). Moreover, we find that all the mixing angles receive positive RGE corrections. From the first panel of Fig. 1, one can observe that the mixing angle θ_{12} is able to achieve the latest best-fit value $\theta_{12} = 33.82^\circ$ as shown by the vertical dashed blue line. Also, shows good agreement with the latest 3σ data. One can understand this behavior from Eq. 5. Within the symmetry, imposing $\rho = \sigma = 90^\circ$, we find that the leading order term of θ_{12} is $\propto (m_2 + m_1)/(m_2 - m_1) > 1$ which enhances the evolution of θ_{12} . On the other hand, θ_{13}, θ_{23} can not reach their current best-fit values i.e., $\theta_{13} = 8.61^\circ$ (see dashed blue horizontal line), $\theta_{23} = 49.6^\circ$ as can be seen from the left and right panels of the first row, respectively. A deviation of less than $\mathcal{O}(1^\circ)$ have been identified for both the parameters. This is because of the suppression factor of ζ term in their respective expressions as given by Eq. 5. However, both the parameters can fit the 3σ global-fit data in a very efficient way [2].

Besides this, for the CP-violating phases, imposing $-\delta = \rho = \sigma = 90^\circ$ in Eqs. 6 as an initial condition, we notice from the first line of Eqs. 6 that the leading order term of the Dirac type CP phase δ is $\ll 1$. Thus, we find less than

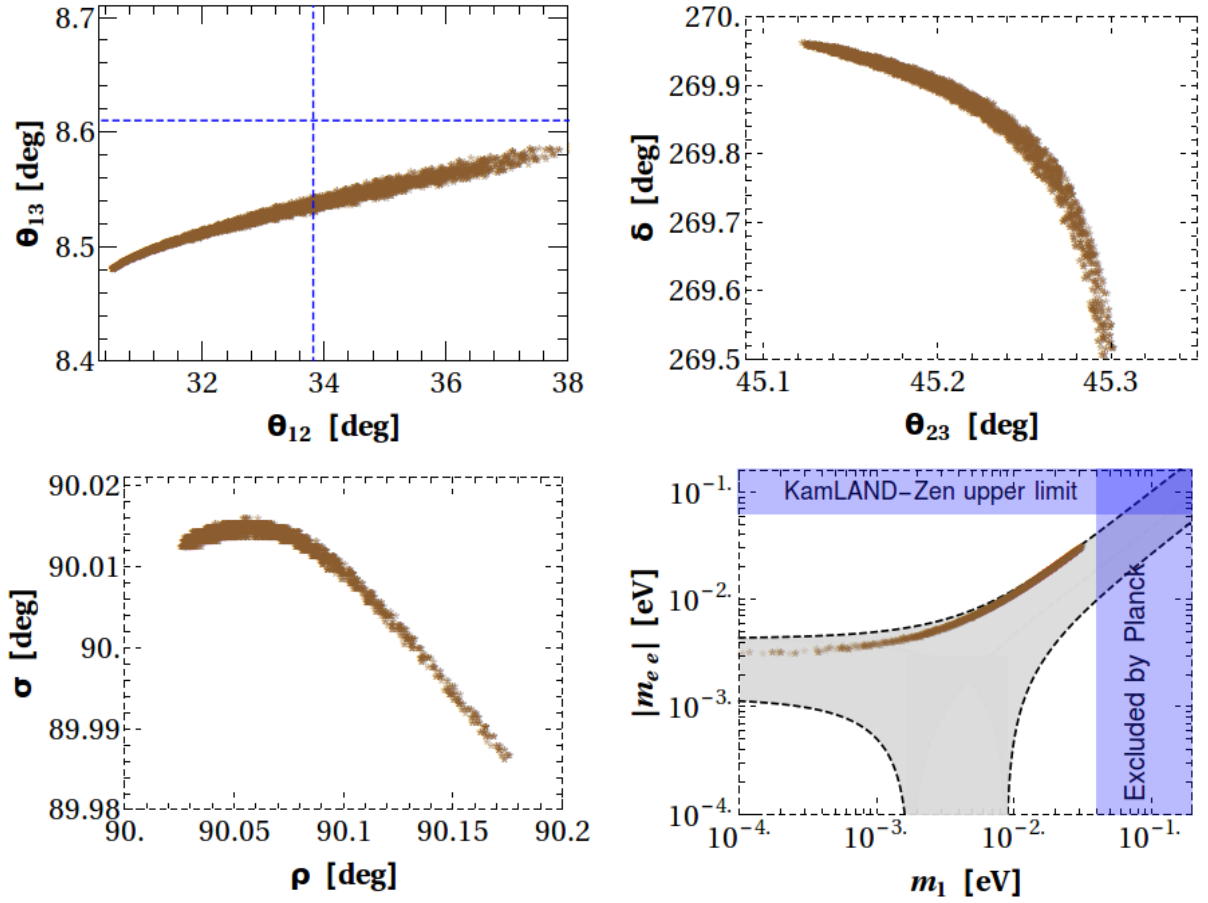


FIG. 1. Correlation plots between different neutrino oscillation parameters at Λ_{EW} . The best-fit values of θ_{13} and θ_{12} are shown by the blue dotted lines in the first panel. The fourth panel shows the prediction for the effective Majorana neutrino mass $|m_{ee}|$. The most stringent upper bound on $|m_{ee}|$ from KamLAND-Zen collaboration are shown by the light blue-horizontal band. The latest result on lightest neutrino mass is shown by the light blue-vertical band from *Planck* Collaboration which gives $\sum m_\nu < 0.12$ eV at the 95% C.L.

$\mathcal{O}(1^\circ)$ deviation for δ from the second panel of Fig. 1. The mild deviation that can be seen from the figure is due to the higher order terms. From the second and third lines of Eqs. 6, we notice that at Λ_{TMM} where initial values i.e., $\theta_{23} = 45^\circ$, $\rho = \sigma = 90^\circ$ have been utilized under the symmetry, the leading order contributions vanishes due to the presence of $(c_{23}^2 - s_{23}^2)$ and $\sin 2\rho, \sin 2\sigma$ terms, respectively. Hence, one expects very mild contributions due to RGE triggered symmetry breaking effect. This has been identified in our numerical study as shown by the first panel of the bottom row of Fig. 1.

In the fourth panel, we show the impact of RGE induced symmetry breaking effect on the neutrinoless double beta ($0\nu\beta\beta$) decay experiments. The $0\nu\beta\beta$ decay $(A, Z) \rightarrow (A, Z + 2) + 2e^-$ is the unique process which can probe the Majorana nature of massive neutrinos. The experiments that are currently searching for the signature of $0\nu\beta\beta$ -decay are GERDA Phase II [22], CUORE [23], SuperNEMO [24], KamLAND-Zen [25] and EXO [26]. However, this process violate lepton number by two-units. The half-life of such decay process is given by [27],

$$(T_{1/2}^{0\nu})^{-1} = G_{0\nu} |M_{0\nu}(A, Z)|^2 |\langle m \rangle_{ee}|^2, \quad (8)$$

where $G_{0\nu}$ stands for two-body phase-space factor, $M_{0\nu}$ is the nuclear matrix element (NME). $|\langle m \rangle_{ee}|$ denotes the effective Majorana neutrino mass. Note that now onwards, we use $|\langle m \rangle_{ee}| = |m_{ee}|$ for simplicity. The expression of $|\langle m \rangle_{ee}|$ is given by,

$$|m_{ee}| = \left| \sum_{i=1}^3 m_i U_{ei}^2 \right|, \quad (9)$$

where U stands for PMNS mixing matrix as mentioned in Eq. (1). In the standard formalism, one can parameterize

$|m_{ee}|$ as

$$|m_{ee}| = |m_1 c_{12}^2 c_{13}^2 e^{2i\rho} + m_2 s_{12}^2 c_{13}^2 e^{2i\sigma} + m_3 s_{13}^2 e^{-2i\delta}|, \quad (10)$$

where $c_{ij}(s_{ij})$ are the leptonic mixing angles, δ , and ρ, σ stand for the Dirac, Majorana CP-phases, respectively. Also, as we have information about the mass-squared differences $\Delta m_{21}^2, \Delta m_{31}^2$ from the neutrino oscillation data, one defines masses m_2, m_3 in terms of the lightest neutrino mass m_1 as $m_2 = \sqrt{m_1^2 + \Delta m_{21}^2}$ and $m_3 = \sqrt{m_1^2 + \Delta m_{21}^2 + \Delta m_{31}^2}$ for the normal mass ordering.

The last panel of Fig. 1 shows the behavior of $|m_{ee}|$. Using the latest 3σ data of oscillation parameters, we present the allowed area by the light-gray color within the dotted-black lines. The RGE-induced breaking pattern within the tetra-maximal mixing pattern has been shown by the brown color⁵. The most stringent upper limit on the effective Majorana neutrino mass $|m_{ee}|$ arises from KamLAND-Zen experiment [25]. Their collaboration have recently reported the bound on $|m_{ee}| < (0.061 - 0.165)$ eV at 90% C.L. by taking into account the uncertainty in the estimation of the nuclear matrix elements, which we show by the horizontal blue band in the fourth panel. On the other hand, the upper bound for the lightest neutrino mass is shown by the vertical blue band. This can be read from the recent *Planck* report [29] which gives $\sum m_\nu < 0.12$ eV (95%, *Planck* TT, TE, EE + lowE + lensing + BAO). One can define $|m_{ee}|$ at Λ_{TMM} within the underlying symmetry by inserting initial values of phases δ, ρ and σ as

$$|m_{ee}|(\Lambda_{\text{TMM}}) = |m_1 c_{12}^2 c_{13}^2 + m_2 s_{12}^2 c_{13}^2 + m_3 s_{13}^2|; \quad \text{for } -\delta = \rho = \sigma = 90^\circ. \quad (11)$$

We notice from Eq. 10 that the cancellation among the various terms of $|m_{ee}|$ depends on the CP-phases. Thus, their breaking patterns at low energies play very important role to understand the numerical results. One sees from Fig. 1 that all the CP-violating phases show less than $\mathcal{O}(1^\circ)$ deviation from their symmetry limit. This tells that there can not be any significant cancellations among the different terms of $|m_{ee}|$ at low energies. This is apparent from Eq. 11 i.e., some components can not attain negative sign with less than $\mathcal{O}(1^\circ)$ deviation, whence there will not be proper cancellations. From the last panel of Fig. 1, we notice that minimum of $|m_{ee}|$ never approaches to zero. We find that $|m_{ee}|$ can reach ~ 2 meV for $m_1 \rightarrow 0.1$ meV. On the other hand, the upper limits of $|m_{ee}|$ can be ~ 35 meV.

III. EXPLICIT BREAKING OF TMM

As observed in previous section that the RGE-induced breaking effect significantly explains the latest best-fit value of the mixing parameter θ_{12} [2]. However, the deviations for θ_{13}, θ_{23} and CP-phases are very mild and less than $\mathcal{O}(1^\circ)$ have been observed, which are much smaller than their latest best-fit values [2]. Although such small deviations are in compatible with current 3σ experimental data, it may become necessary to consider large deviations when more accurate data will be included. In this section, we discuss the breaking of tetra-maximal mixing pattern to explain the low energy data by introducing explicit breaking terms in the neutrino mixing matrix.

We introduce explicit breaking terms in such a way that one can explain large θ_{12} as well as non-maximal values of θ_{23} and δ , which are in well agreement with the latest global analysis data [2, 9, 10]. Moreover, although the predicted θ_{13} within this mixing pattern is in compatible with the latest 3σ data, we show that such explicit breaking can also explain its best-fit value. Introducing breaking terms in 1-2, 2-3 rotation matrices, one can re-write Eq. 2 as

$$V' = P_l \otimes O_{23} \left(\frac{\pi}{4}, \frac{\pi}{2} + \delta_\epsilon \right) \otimes O_{13} \left(\frac{\pi}{4}, 0 \right) \otimes O_{12} \left(\frac{\pi}{4} + \epsilon_{12}, 0 \right) \otimes O_{13} \left(\frac{\pi}{4}, \pi \right), \quad (12)$$

where $\delta_\epsilon, \epsilon_{12}$ are the explicit breaking parameters. Expanding Eq. 12 upto leading order terms, we get

$$V' = V_0 + \frac{1}{4}\epsilon_{12} \begin{pmatrix} -\sqrt{2} & 2 & \sqrt{2} \\ -\sqrt{2}-i & -2+i\sqrt{2} & \sqrt{2}+i \\ -\sqrt{2}+i & -2-i\sqrt{2} & \sqrt{2}-i \end{pmatrix} + \frac{1}{4}\delta_\epsilon \begin{pmatrix} 0 & 0 & 0 \\ 1-\sqrt{2} & \sqrt{2} & -1-\sqrt{2} \\ i\sqrt{2} & i2 & i\sqrt{2} \end{pmatrix} + \mathcal{O}(\epsilon_{13}^2, \delta_\epsilon^2, \epsilon_{13}\delta_\epsilon). \quad (13)$$

It is clear from Eq. 13 that if one considers perturbative terms $\epsilon_{12} \neq 0, \delta_\epsilon = 0$ in such scenario Eq. 13 does not serve our intention to explain large θ_{12} together with non-maximal θ_{23} , and δ . As in absence of δ_ϵ , one can see that $|V'_{\mu i}| = |V'_{\tau i}|$

⁵ Recently, the pattern of $|m_{ee}|$ due to RGE corrections within the framework of $\mu - \tau$ reflection symmetry have been discussed in [28].

is still maintained and hence maximality remain preserved for θ_{23} , and δ . However, non-zero δ_ϵ breaks this equality and able to give non-maximal values of θ_{23} , δ . In order to have better understanding, we calculate mixing angles and Jarlskog invariant J_{CP} as

$$\begin{aligned}\sin^2 \theta_{13} &= \frac{1}{8}(3 - 2\sqrt{2}) + \frac{1}{4}(\sqrt{2} - 1)\epsilon_{12} + \mathcal{O}(\epsilon_{12}^2), \\ \sin^2 \theta_{12} &= \frac{2}{5 + 2\sqrt{2}} + \frac{4}{289}(12 + 19\sqrt{2})\epsilon_{12} + \mathcal{O}(\epsilon_{12}^2), \\ \sin^2 \theta_{23} &= \frac{1}{2} - \frac{1}{17}(6 + \sqrt{2})\sin \delta_\epsilon - \frac{2}{289}(45 - \sqrt{2})\epsilon_{12}\sin \delta_\epsilon + \mathcal{O}(\epsilon_{12}^2, \delta_\epsilon^2), \\ J_{CP} &= -\frac{1}{32}(1 + 3\epsilon_{12} + \frac{3}{2}\epsilon_{12}^2 - \frac{1}{2}\delta_\epsilon^2) + \mathcal{O}(\epsilon_{12}^2\delta_\epsilon^2).\end{aligned}\tag{14}$$

Note that in calculating last two expressions, we kept next-to-leading order terms.

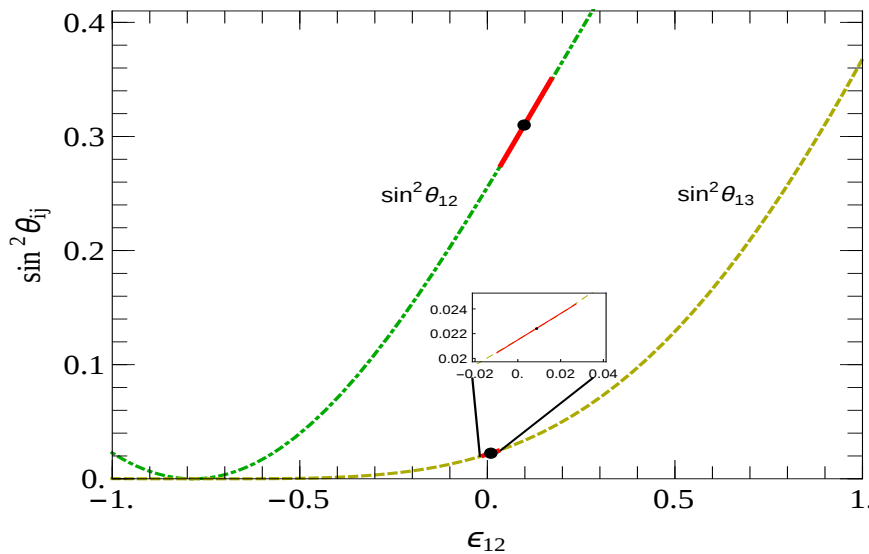


FIG. 2. Correlations between $\sin^2 \theta_{12}$, $\sin^2 \theta_{13}$ vs ϵ_{12} are shown by the dark green (dash-dotted) and light green (dashed) lines, respectively. The red color patch and black-dot represent 3σ allowed region and best-fit value of the latest data, respectively.

From Fig. 2, we notice that an infinitesimal value of ϵ_{12} is able to explain the whole 3σ range of the mixing angle θ_{13} (see the dashed light green curve). The latest 3σ range of θ_{13} is shown by the red color patch, where as the best-fit value is marked by the black dot. The dashed-dotted dark green curve shows our numerical results for θ_{12} . One can see that $\epsilon_{12} \sim 0.1$ is able to generate the latest best-fit value of θ_{12} , which is marked by the black dot, whereas $\epsilon_{12} \sim 0.18$ is able to explain the current 3σ range of θ_{12} as shown by the red patch.

We shown the impact of explicit breaking terms on the oscillation parameters θ_{23} , and δ in Fig. 3. As we know that any non-zero values of δ_ϵ will lead to non-maximal values of θ_{23} , and δ , which is apparent from the figure. The best-fit and the 3σ range of the latest global analysis of neutrino oscillation data are shown by the black dash and the blue dash lines, respectively. We notice from the left panel figure that an infinitesimal value of δ_ϵ is able to generate the latest best-fit value of θ_{23} (see the intersection point between the brown curve and the blue dash curve). On the other hand, it can be seen from the right panel figure that any value of δ_ϵ are unable to explains the latest best-fit value of δ_{CP} . However, this explicit breaking term can explain the values of δ_{CP} which lies within the current 3σ data.

IV. SUMMARY

We study here tetra-maximal neutrino mixing pattern, which was originally proposed in [14], to address the latest global analysis of neutrino oscillation data. This symmetry predicts with $\theta_{12} \approx 30.4^\circ$, $\theta_{13} \approx 8.4^\circ$, $\theta_{23} = 45^\circ$ and

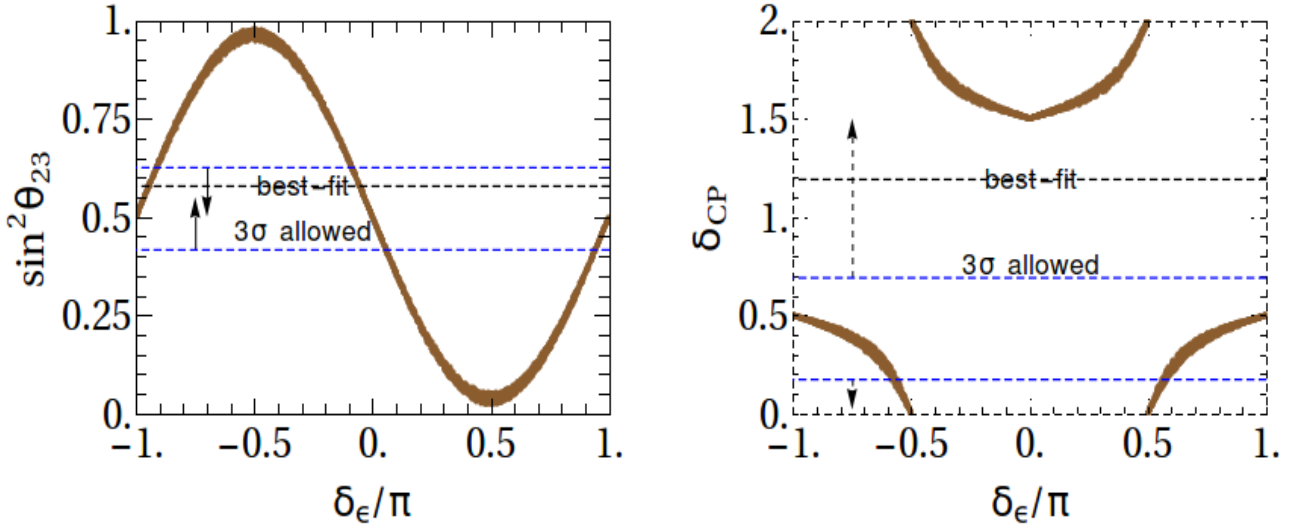


FIG. 3. Left: Correlation between $\sin^2 \theta_{23}$ vs δ_ϵ as shown by the brown curve. Right: Correlation between δ_{CP} vs δ_ϵ as shown by the brown curve. The black dash and the blue dash lines show the latest best-fit value and the 3σ range, respectively.

$-\delta = \rho = \sigma = 90^\circ$. According to the latest global analysis of neutrino oscillation data [2, 9, 10], one can notice relatively higher best-fit value of θ_{12} as well as non-maximal values of both θ_{23} , and δ . Besides this, though the latest T2K results are in good agreement with the symmetry, the current NO ν A results seem to favor non-maximal θ_{23} , and δ . In order to explain the realistic data, we study the breaking of TMM pattern. Here we examine the status of tetra-maximal neutrino mixing pattern for the leptonic mixing matrix by confronting them with current neutrino oscillation data. To do that we first examine the breaking of the symmetry due to renormalization group running effects and then study the impact of explicit breaking term.

From the RGE-induced symmetry breaking we find less than $\mathcal{O}(1^\circ)$ deviations for the mixing parameters θ_{13}, θ_{23} from their predicted values. A significantly large deviation of θ_{12} has been identified. These numerical results are in good agreement with the analytical expressions as described in Fig. 2. Besides this, for all the three CP-phases less than $\mathcal{O}(1^\circ)$ deviations have been observed. We also study the impact of RGE-induced symmetry breaking on the effective Majorana neutrino mass matrix, $|\langle m \rangle_{ee}|$. It has been found that minimum of $|\langle m \rangle_{ee}|$ can never reach to zero in this framework. We also notice that $|m_{ee}|$ can reach ~ 2 meV for $m_1 \rightarrow 0.1$ meV and the upper limits of $|m_{ee}|$ can be as large as ~ 35 meV. Finally, we discuss the breaking of the symmetry in presence of explicit breaking terms. In this approach, we are able to generate large deviations for the leptonic flavor mixing parameters θ_{13}, θ_{23} and δ for a relatively small values of the breaking terms. We summarize these results in Fig. 3.

V. ACKNOWLEDGEMENTS

Author is supported by the postdoctoral fellowship program DGAPA-UNAM. This work is also supported by the grants CONACYT CB-2017-2018/A1-S-13051 (México) and the German-Mexican research collaboration grant SP 778/4-1 (DFG) and 278017 (CONACYT).

-
- [1] M. Tanabashi *et al.* (Particle Data Group), *Phys. Rev.* **D98**, 030001 (2018).
 - [2] I. Esteban, M. C. Gonzalez-Garcia, A. Hernandez-Cabezudo, M. Maltoni, and T. Schwetz, *JHEP* **01**, 106 (2019), [arXiv:1811.05487 \[hep-ph\]](#).
 - [3] G. Altarelli and F. Feruglio, *Rev. Mod. Phys.* **82**, 2701 (2010), [arXiv:1002.0211 \[hep-ph\]](#).
 - [4] G. Altarelli, F. Feruglio, and L. Merlo, *Fortsch. Phys.* **61**, 507 (2013), [arXiv:1205.5133 \[hep-ph\]](#).
 - [5] A. Yu. Smirnov, *Proceedings, 2nd Symposium on Prospects in the Physics of Discrete Symmetries (DISCRETE 2010): Rome, Italy, December 6-11, 2010*, *J. Phys. Conf. Ser.* **335**, 012006 (2011), [arXiv:1103.3461 \[hep-ph\]](#).

- [6] H. Ishimori, T. Kobayashi, H. Ohki, Y. Shimizu, H. Okada, and M. Tanimoto, *Prog. Theor. Phys. Suppl.* **183**, 1 (2010), [arXiv:1003.3552 \[hep-th\]](#).
- [7] S. F. King and C. Luhn, *Rept. Prog. Phys.* **76**, 056201 (2013), [arXiv:1301.1340 \[hep-ph\]](#).
- [8] P. F. Harrison, D. H. Perkins, and W. G. Scott, *Phys. Lett.* **B530**, 167 (2002), [arXiv:hep-ph/0202074 \[hep-ph\]](#).
- [9] F. Capozzi, E. Lisi, A. Marrone, D. Montanino, and A. Palazzo, *Nucl. Phys.* **B908**, 218 (2016), [arXiv:1601.07777 \[hep-ph\]](#).
- [10] P. F. de Salas, D. V. Forero, C. A. Ternes, M. Tortola, and J. W. F. Valle, (2017), [arXiv:1708.01186 \[hep-ph\]](#).
- [11] P. F. Harrison and W. G. Scott, *Phys. Lett.* **B547**, 219 (2002), [arXiv:hep-ph/0210197 \[hep-ph\]](#).
- [12] Z.-z. Xing and Z.-h. Zhao, *Rept. Prog. Phys.* **79**, 076201 (2016), [arXiv:1512.04207 \[hep-ph\]](#).
- [13] N. Nath, *Phys. Rev.* **D98**, 075015 (2018), [arXiv:1805.05823 \[hep-ph\]](#).
- [14] Z.-z. Xing, *Phys. Rev.* **D78**, 011301 (2008), [arXiv:0805.0416 \[hep-ph\]](#).
- [15] H. Zhang and S. Zhou, *Phys. Lett.* **B704**, 296 (2011), [arXiv:1107.1097 \[hep-ph\]](#).
- [16] K. Abe *et al.* (T2K), *Phys. Rev. Lett.* **118**, 151801 (2017), [arXiv:1701.00432 \[hep-ex\]](#).
- [17] A. Radovic *et al.* (NO ν A) (2018) talk given at the Fermilab, January 2018, USA, <http://nova-docdb.fnal.gov/cgi-bin/ShowDocument?docid=25938>.
- [18] E. Majorana, *Nuovo Cim.* **14**, 171 (1937).
- [19] P. H. Chankowski and Z. Pluciennik, *Phys. Lett.* **B316**, 312 (1993), [arXiv:hep-ph/9306333 \[hep-ph\]](#); K. S. Babu, C. N. Leung, and J. T. Pantaleone, *Phys. Lett.* **B319**, 191 (1993), [arXiv:hep-ph/9309223 \[hep-ph\]](#); S. Antusch, M. Drees, J. Kersten, M. Lindner, and M. Ratz, *Phys. Lett.* **B519**, 238 (2001), [arXiv:hep-ph/0108005 \[hep-ph\]](#); M. A. Schmidt, *Phys. Rev.* **D76**, 073010 (2007), [Erratum: *Phys. Rev.* **D85**, 099903(2012)], [arXiv:0705.3841 \[hep-ph\]](#); J. Chakraborty, A. Dighe, S. Goswami, and S. Ray, *Nucl. Phys.* **B820**, 116 (2009), [arXiv:0812.2776 \[hep-ph\]](#); M. Blennow, H. Melbeus, T. Ohlsson, and H. Zhang, *JHEP* **04**, 052 (2011), [arXiv:1101.2585 \[hep-ph\]](#).
- [20] S. Antusch, J. Kersten, M. Lindner, and M. Ratz, *Nucl. Phys.* **B674**, 401 (2003), [arXiv:hep-ph/0305273 \[hep-ph\]](#).
- [21] F. Feroz and M. P. Hobson, *Mon. Not. Roy. Astron. Soc.* **384**, 449 (2008), [arXiv:0704.3704 \[astro-ph\]](#); F. Feroz, M. P. Hobson, and M. Bridges, *Mon. Not. Roy. Astron. Soc.* **398**, 1601 (2009), [arXiv:0809.3437 \[astro-ph\]](#); F. Feroz, M. P. Hobson, E. Cameron, and A. N. Pettitt, (2013), [arXiv:1306.2144 \[astro-ph.IM\]](#).
- [22] M. Agostini *et al.* (GERDA), *Phys. Rev. Lett.* **120**, 132503 (2018), [arXiv:1803.11100 \[nucl-ex\]](#).
- [23] C. Alduino *et al.* (CUORE), *Phys. Rev. Lett.* **120**, 132501 (2018), [arXiv:1710.07988 \[nucl-ex\]](#).
- [24] A. S. Barabash, *Proceedings, 12th International Conference on Topics in Astroparticle and Underground Physics (TAUP 2011): Munich, Germany, September 5-9, 2011*, *J. Phys. Conf. Ser.* **375**, 042012 (2012), [arXiv:1112.1784 \[nucl-ex\]](#).
- [25] A. Gando *et al.* (KamLAND-Zen), *Phys. Rev. Lett.* **117**, 082503 (2016), [Addendum: *Phys. Rev. Lett.* **117**, no.10, 109903(2016)], [arXiv:1605.02889 \[hep-ex\]](#).
- [26] M. Agostini, G. Benato, and J. Detwiler, *Phys. Rev.* **D96**, 053001 (2017), [arXiv:1705.02996 \[hep-ex\]](#).
- [27] W. Rodejohann, *Int. J. Mod. Phys.* **E20**, 1833 (2011), [arXiv:1106.1334 \[hep-ph\]](#); P. S. Bhupal Dev, S. Goswami, M. Mitra, and W. Rodejohann, *Phys. Rev.* **D88**, 091301 (2013), [arXiv:1305.0056 \[hep-ph\]](#).
- [28] N. Nath, Z.-z. Xing, and J. Zhang, *Eur. Phys. J.* **C78**, 289 (2018), [arXiv:1801.09931 \[hep-ph\]](#); N. Nath, *Phys. Rev.* **D99**, 035026 (2019), [arXiv:1810.07938 \[hep-ph\]](#).
- [29] N. Aghanim *et al.* (Planck), (2018), [arXiv:1807.06209 \[astro-ph.CO\]](#).